

Electronic Supplementary Information

Preparation of nano-MFI zeolites doped with Al/Ti and their performance for VOCs sorption

Xiaolong Wang^{a, b}, Donghang Chen^{a, b}, Yongsheng Jia^c, Zhongyu Jiang^{a, b}, Kongzhai Li^d,
Soamwadee Chaianansutcharit^e, Prasert Reubroycharoen^f and Limin Guo^{a, b, *}

^aSchool of Environmental Science and Engineering, Huazhong University of Science and
Technology, Wuhan 430074, China

^bHubei Key Laboratory of Multi-media Pollution Cooperative Control in Yangtze Basin,
School of Environmental Science & Engineering, Huazhong University of Science and
Technology, Wuhan, 430074, China

^cState Key Laboratory of Advanced Electromagnetic Engineering and Technology, School of
Electrical and Electronic Engineering, Huazhong University of Science and Technology, Wuhan
430074, China

^dFaculty of Metallurgical and Energy Engineering, Kunming University of Science and
Technology, Kunming 650093, China

^eDepartment of Chemistry, Faculty of Science, Chulalongkorn University, Bangkok 10330,
Thailand

^fDepartment of Chemical Technology, Faculty of Science, Chulalongkorn University,
Bangkok 10330, Thailand

*Corresponding author.

E-mail: limguo@hust.edu.cn (Limin Guo).

Characterization

The powder X-ray diffraction (XRD) patterns were obtained on a Shimadzu XRD-7000 diffractometer. Fourier transform infrared spectroscopy (FTIR) was conducted on a Bruker Tensor II spectrometer. The N₂ sorption measurements of the samples were carried out by a Micromeritics Tristar II 3020 at 77 K. Field emission scanning electron microscopic (FE-SEM) observation was performed on a Nova Nano SEM 450 field emission scanning electron microscopy. Transmission Electron Microscopy (TEM) images were collected using a Talos F200X TEM. The ammonia temperature-programmed desorption (NH₃-TPD) was carried out by an autocatalytic adsorption system (VDSorb-91i, Vodo). The actual Si/M (M = Al or Ti) ratios were tested by X-ray Fluorescence (XRF, AXIOSmAX) analysis.

Dynamic adsorption testing

Dynamic adsorption measurements were carried out using a fixed-bed reactor equipped with a gas chromatography (GC) apparatus with the hydrogen flame ion detector (FID). 0.1 g of 40-60 mesh sample particles were packed into a quartz tube with an internal diameter of 4 mm. 400 ppm toluene or 558 ppm acetone balanced by N₂ (80%) and O₂ (20%) at a mass flow rate of 100 mL min⁻¹ was fed into a fixed-bed quartz tube reactor at 303 K. The tested samples were treated under N₂ flow at 573 K for 1 hour before measurement. The sampling interval was 2 minutes. When testing the adsorption properties of samples in the presence of water, the water vapor bubble bottle was used, and the relative humidity was controlled to be 50% by bubbling N₂ at a flow rate of 50 mL min⁻¹ into the water. The dynamic adsorption capacity (q) of the sample is calculated according to equation (1).

$$q = \frac{F * C_0 * 10^{-6}}{W} \left[t_s - \int_0^{t_s} \frac{C_t}{C_0} dt \right] \quad (1)$$

where q (mg/g) is the dynamic adsorption capacity of the sample, F (mL/min) is the gas flow rate, C₀ (mg/L) is the initial concentration of VOCs, C_t (mg/L) is the concentration of VOCs monitored by GC at time t, W (g) is the adsorbent mass, t (min)

is the adsorption time, and t_s (min) is the time to reach adsorption equilibrium.

Adsorption-desorption cycle test

Utilizing an adsorption-desorption cycle test, the cyclic regeneration effectiveness of the samples was determined. Gas chromatography with FID was used to monitor the variations in VOCs content during adsorption and desorption during the sample adsorption-desorption cycling test. For each experiment, 0.1 g of 40-60 mesh adsorbent was inserted into a quartz tube and pretreated for one hour at 573 K. After the temperature was lowered to 303 K, 400 ppm of VOCs gas was added. As soon as the sample attained adsorption equilibrium, the VOCs were separated from the adsorbed gas, and the adsorbent fixed bed was heated to 573 K at a rate of $10 \text{ K}\cdot\text{min}^{-1}$ for one hour. After desorption was complete, the adsorbent was carried out adsorption and desorption process five times without replacement under the same conditions of saturation and desorption.

Temperature-programmed desorption measurements

Temperature-programmed desorption of toluene (Toluene-TPD) and acetone (Acetone-TPD) measurements were carried out at different heating rates from 4 K/min to 10 K/min. The signal of toluene was detected by online mass spectrometry (MS, Hiden HPR 20). For each test, 0.1 g of 40-60 mesh adsorbent was weighed and put into a quartz tube. It was heated at 573 K for an hour to remove moisture and impurities while being purged with a 100 mL/min stream of high-purity argon gas. The sample was then cooled to room temperature. After the samples were adsorbed with 1000 ppm VOCs to saturation at room temperature, it was cleaned for one hour with argon gas to get rid of the VOCs that had stuck to its surface. The ramp-up program was then set, and the change in VOCs during desorption was measured.

Based on the desorption peak temperatures of TPD curves at different heating rates, the active energy between toluene and samples was calculated by the following equation.

$$\ln \left(\frac{RT_p^2}{\beta_H} \right) = \frac{E}{R} \cdot \frac{1}{T_p} + \ln \left(\frac{E}{k_0} \right) \quad (2)$$

Where R (J/ (kg. K)) is the gas constant, T_p (K) is the desorption peak temperature of the TPD curves under different heating rates, β_H (K/min) is the heating rate, E (kJ/mol) is the active energy between toluene and the sample, and k_0 is the desorption rate coefficient.

Adsorption kinetics

The intra-particle diffusion model assumes that the effect of the diffusion of VOCs is the rate-controlling step for the sorption process, the intra-particle diffusivity is constant and the direction of the diffusion is radial¹. This model was used to calculate the intraparticle diffusion rate constant. The model equation is expressed by the following equation:

$$q_t = k_{id}t^{\frac{1}{2}} + C \quad (3)$$

where q_t is the amount of VOCs sorbed at time t , k_{id} is the intraparticle diffusion rate constant, 't' is the time and the value of 'C' is proportional to the boundary layer.

Pseudo-first-order model, derived from mass balance equation, which can accurately describe external mass transfer process and predict equilibrium adsorption capacity. The expression of this model is generally expressed as follows²:

$$q_t = q_e[1 - \exp(-k_1t)] \quad (4)$$

where q_t and q_e are the amount of VOCs sorbed at time t and at equilibrium and k_1 is the rate constant of pseudo-first-order equation.

The pseudo-second-order model assumes that the sorption process is a pseudo-chemical reaction process. This model constitutes a mass action rate model where the surface diffusivity is inversely proportional to the square of concentration of vacant sites on the surface³. The equation is expressed by the following equation:

$$q_t = \frac{k_2q_e^2t}{1 + k_2q_e t} \quad (5)$$

where q_e and q_t are the amount of VOCs adsorbed at equilibrium and at time t , k_2 is the pseudo-second order constant and t is the time.

The Elovich model is based on the Temkin isotherm equation, which is commonly

used to describe the chemical adsorption of gases on solid surfaces. The Elovich equation⁴ is expressed as:

$$q_t = \frac{1}{b} \ln(a \times b) + \frac{1}{b} \ln t \quad (6)$$

where q_t is the amount of VOCs adsorbed at equilibrium and at time t , a is regarded as the initial rate, b is related to the extent of surface, coverage and activation energy for chemisorption⁴.

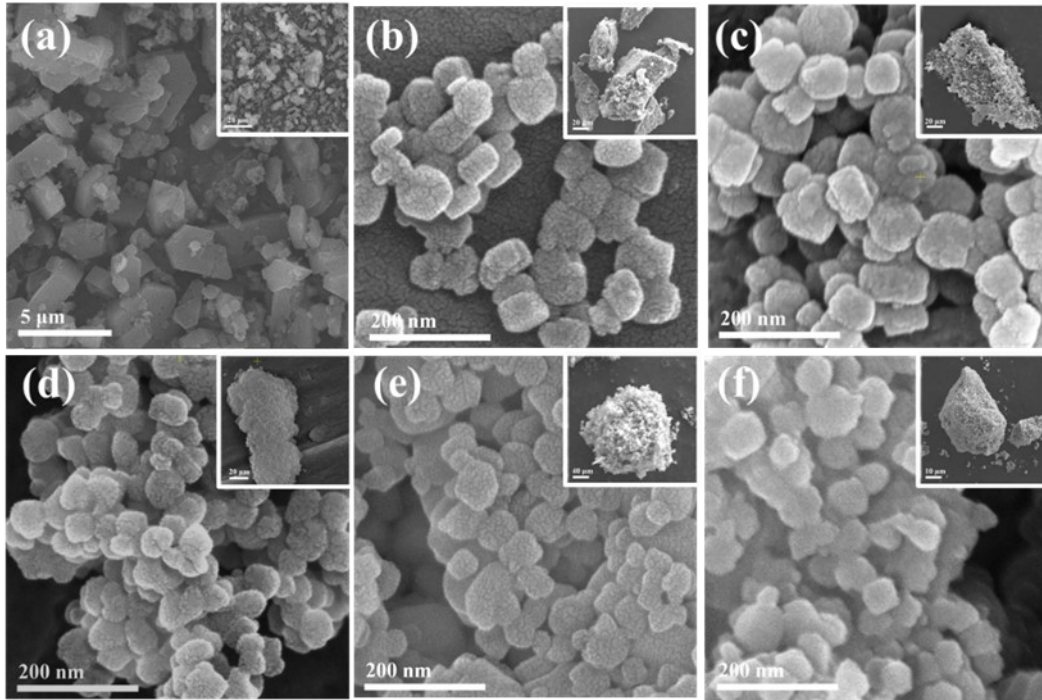


Fig. S1. SEM images of MFI zeolites ((a) CM-Al-23, (b) NM-Si, (c) NM-Ti-84, (d) NM-Ti/Al, (e) NM-Al-87, (f) NM-Al-41)

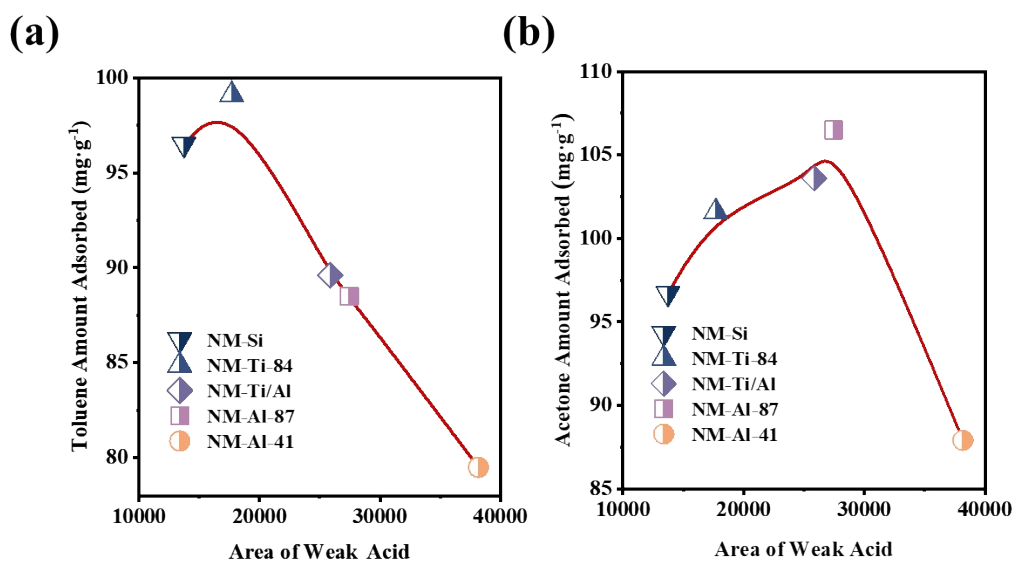


Fig. S2. The plot of the relationship between the adsorption of zeolite under dry gas condition and the content of weak acids in MFI zeolites

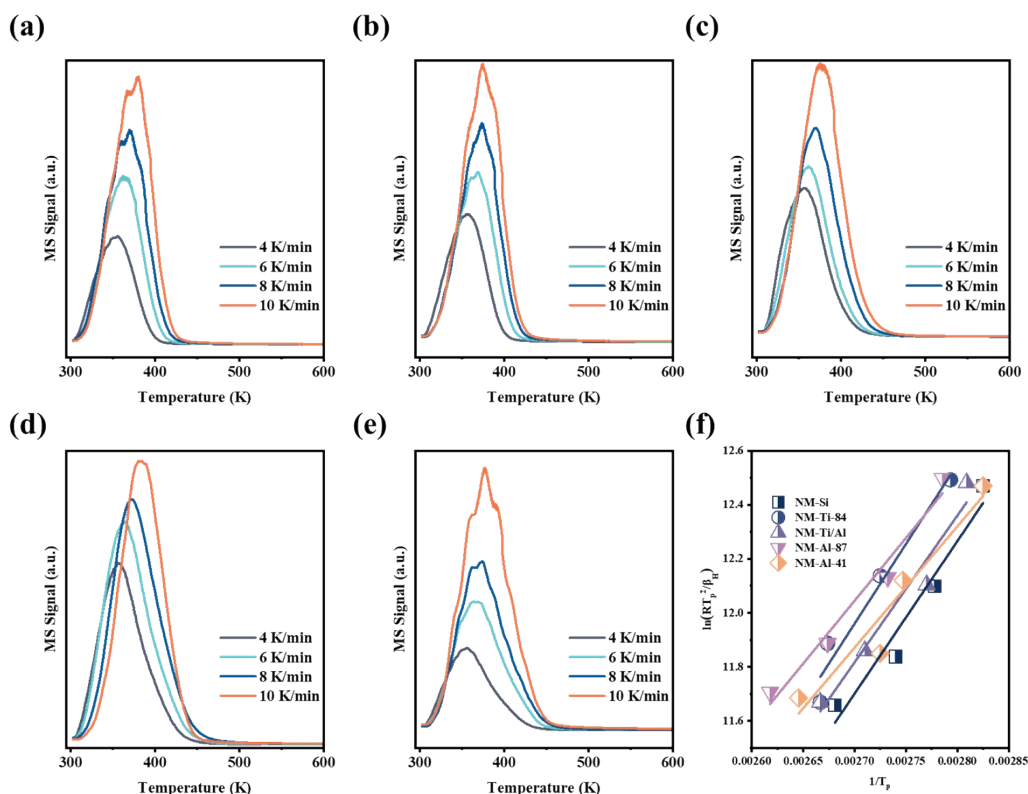


Fig. S3. Temperature-programmed toluene desorption measurements under different β_H on NM-Si (a), NM-Ti-84 (b), NM-Ti/Al (c), NM-Al-87 (d), and NM-Al-41 (e) and the linear fitting between $\ln(RT_p^2/\beta_H)$ and $1/T_p$ (f).

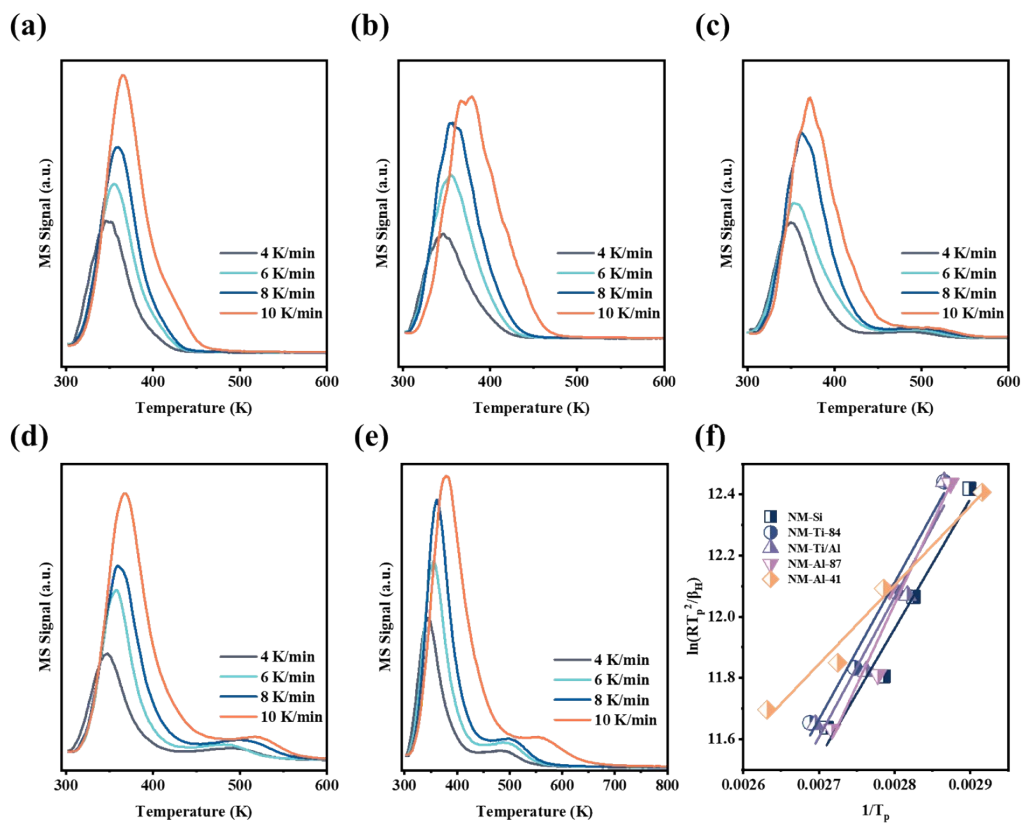


Fig. S4. Temperature-programmed acetone desorption measurements under different β_H on NM-Si (a), NM-Ti-84 (b), NM-Ti/Al (c), NM-Al-87 (d), and NM-Al-41 (e) and the linear fitting between $\ln(RT_p^2/\beta_H)$ and $1/T_p$ (f).

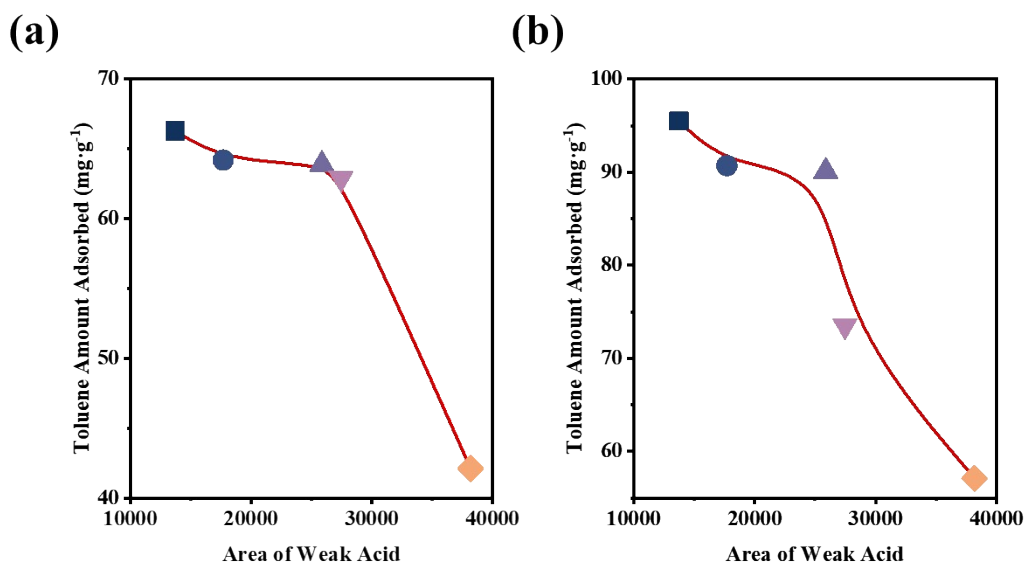


Fig. S5. The plot of the relationship between the adsorption of zeolite under wet gas condition and the content of weak acids in MFI zeolites.

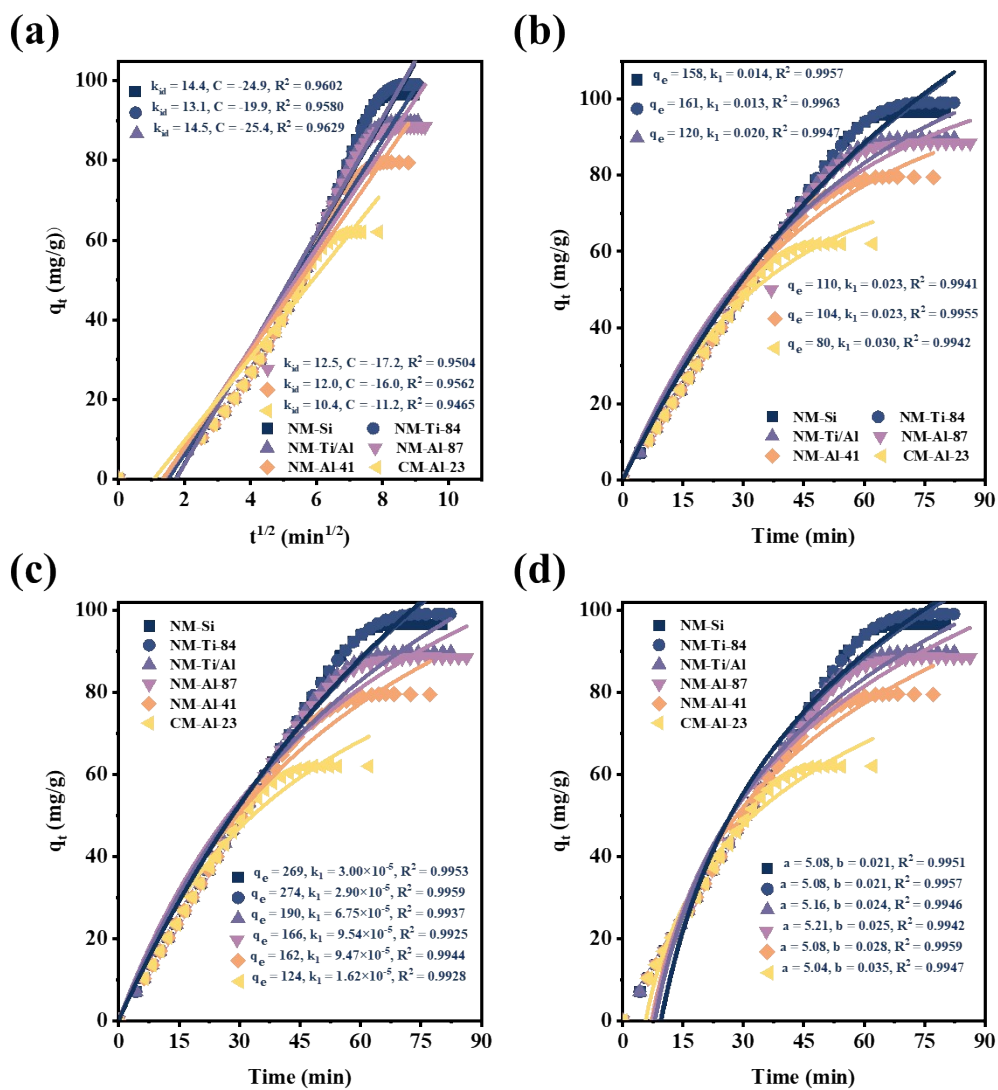


Fig. S6. Linear plots of different kinetic models for toluene sorption onto MFI zeolites (a: Intra-particle diffusion model; b: Pseudo-first-order model; c: Pseudo-second-order model; d: Elovich model).

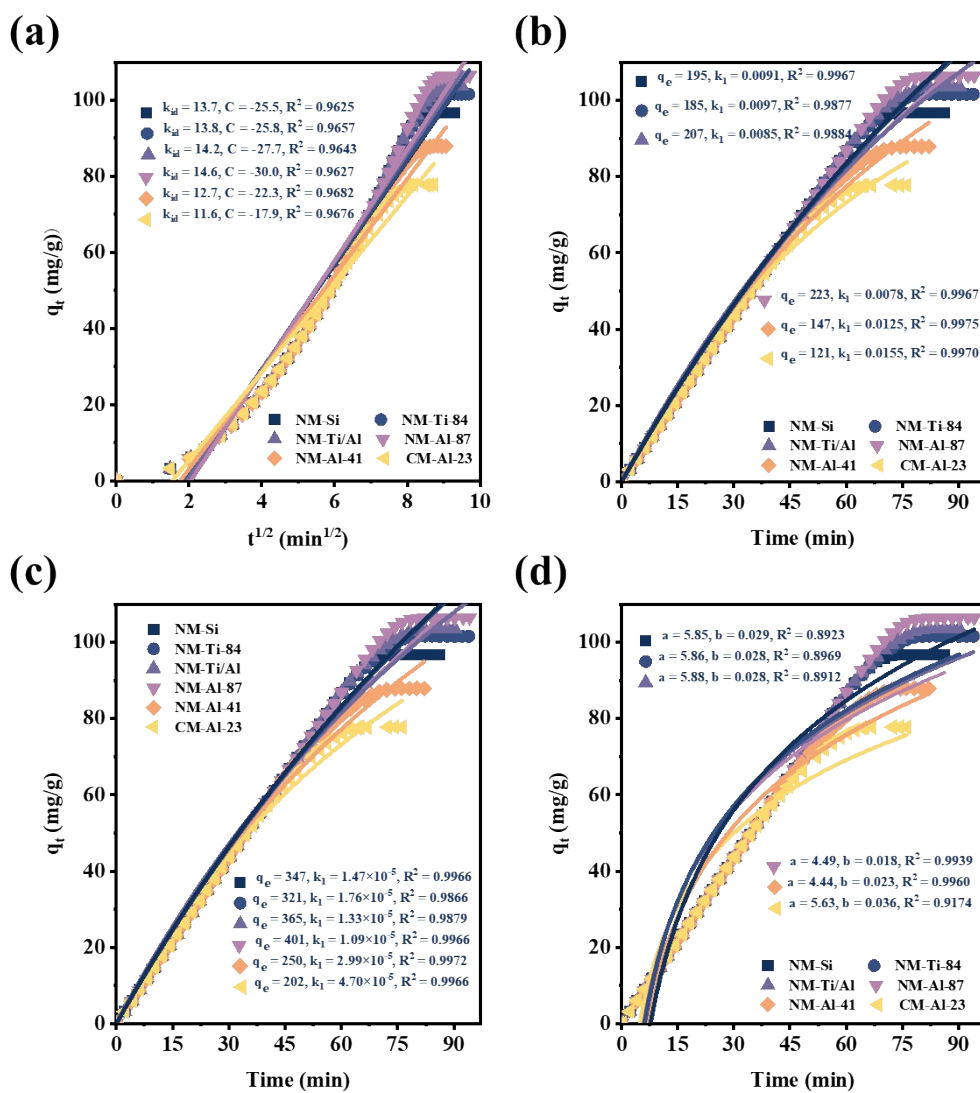
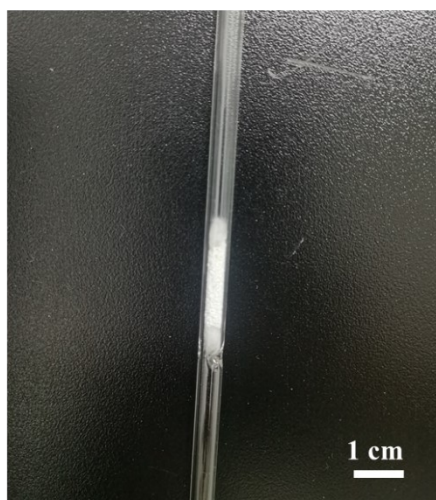


Fig. S7. Linear plots of different kinetic models for acetone sorption onto MFI zeolites (a: Intra-particle diffusion model; b: Pseudo-first-order model; c: Pseudo-second-order model; d: Elovich model).

(a)



(b)

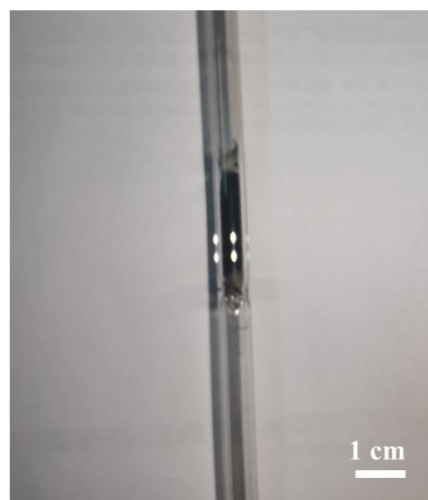


Fig. S8. Digital images of NM-Al-41 before (a) and after (b) cyclic acetone sorption.

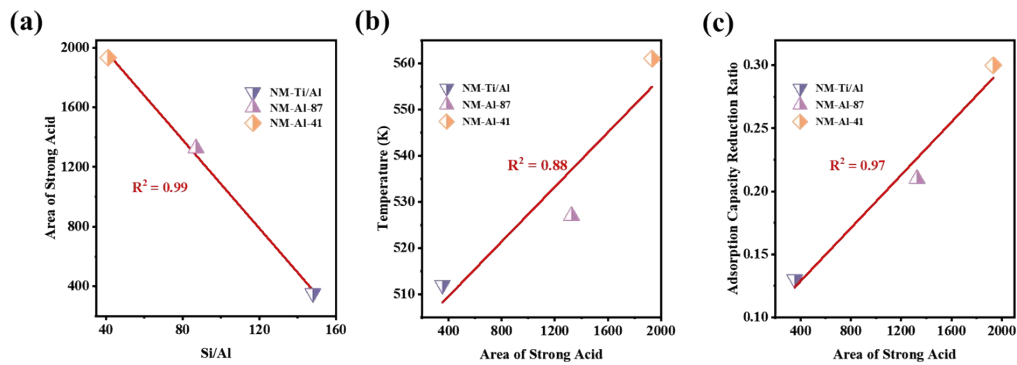


Fig. S9. The plots of the strong acid peak areas of NM-Ti/Al, NM-Al-87 and NM-Al-41 as a function of the Si/Al(a), the temperatures corresponding to the second desorption peak of acetone-TPD (b), and the adsorption capacity reduction ratio (c).

Table S1. The MFI zeolites synthesis conditions

Sample	TEOS (g)	TPAOH (g)	H ₂ O (mL)	Seed (g)	Urea (g)	AIP (g)	TBOT (g)	Crystallization temperature and time (K and day)
NM-Si	2.8	4.5	4.6	6.2	0.5	/	/	453 (1 day)
NM-Ti-84	2.8	4.5	4.6	6.2	0.5	/	0.109	453 (1 day)
NM-Ti/Al	2.8	4.5	4.6	6.2	0.5	0.033	0.054	453 (1 day)
NM-Al-87	2.8	4.5	4.6	6.2	0.5	0.065	/	453 (1 day)
NM-Al-41	2.8	4.5	4.6	6.2	0.5	0.130	/	453 (1 day)

Table S2. The breakthrough time and adsorption capacity of MFI zeolites

Samples	Toluene		Toluene	
	Breakthrough	Adsorption	Breakthrough	Adsorption
	time (min)	capacity (mg·g ⁻¹)	time (min)	capacity (mg·g ⁻¹)
NM-Si	46	96.5	58	96.7
NM-Ti-84	46	99.1	58	101.6
NM-Ti/Al	40	89.6	60	103.6
NM-Al-87	36	88.5	66	106.5
NM-Al-41	30	79.5	42	87.9
CM-Al-23	22	62.0	34	77.8

Table S3. Desorption interaction energy, E_d and peak temperature T_p of toluene on MFI zeolites

Samples	Value of T_p (K) for peaks of TPD curve obtained at				E_d (kJ/mol)	R^2
	heating rate, β_H					
	4 (K/min)	6 (K/min)	8 (K/min)	10 (K/min)		
NM-Si	354	360	365	373	47.0	0.95
NM-Ti-84	358	367	374	375	49.1	0.96
NM-Ti/Al	356	361	369	375	45.2	0.96
NM-Al-87	359	366	374	382	38.7	0.97
NM-Al-41	354	364	367	378	37.3	0.93

Table S4. Desorption interaction energy, E_d and peak temperature T_p of acetone on MFI zeolites

Samples	Value of T_p (K) for peaks of TPD curve obtained at				E_d (kJ/mol)	R^2
	heating rate, β_H					
	4 (K/min)	6 (K/min)	8 (K/min)	10 (K/min)		
NM-Si	356	364	371	380	35.3	0.97
NM-Ti-84	356	368	374	375	37.2	0.99
NM-Ti/Al	356	362	370	377	38.1	0.94
NM-Al-87	357	364	396	402	44.1	0.95
NM-Al-41	354	364	373	377	25.9	0.98

Table S5. Kinetic data and correlation coefficient R^2 obtained from intraparticle diffusion model

Sample	Toluene			Acetone		
	k_{id}	C	R^2	k_{id}	C	R^2
	($\text{mg}/\text{g}_{\text{ads}} \cdot \text{min}^{1/2}$)	($\text{mg}/\text{g}_{\text{ads}}$)		($\text{mg}/\text{g}_{\text{ads}} \cdot \text{min}^{1/2}$)	($\text{mg}/\text{g}_{\text{ads}}$)	
NM-Si	14.4	-24.9	0.9602	13.7	-25.5	0.9625
NM-Ti-84	13.1	-19.9	0.9580	13.8	-25.8	0.9657
NM-Ti/Al	14.5	-25.4	0.9629	14.2	-27.7	0.9643
NM-Al-87	12.5	-17.2	0.9504	14.6	-30.0	0.9627
NM-Al-41	12.0	-16.0	0.9562	12.7	-22.3	0.9682
CM-Al-23	10.4	-11.2	0.9465	11.6	-17.9	0.9676

Table S6. Kinetic data and correlation coefficient R^2 obtained from pseudo-first order kinetic model

Sample	Toluene			Acetone		
	q_e (mg/g _{ads})	k_1 (min ⁻¹)	R^2	q_e (mg/g _{ads})	k_1 (min ⁻¹)	R^2
NM-Si	158	0.014	0.9957	195	0.0091	0.9967
NM-Ti-84	161	0.013	0.9963	185	0.0097	0.9877
NM-Ti/Al	120	0.020	0.9947	207	0.0085	0.9884
NM-Al-87	110	0.023	0.9941	223	0.0078	0.9967
NM-Al-41	104	0.023	0.9955	147	0.0125	0.9975
CM-Al-23	80	0.030	0.9942	121	0.0155	0.9970

Table S7. Kinetic data and correlation coefficient R^2 obtained from pseudo-second order kinetic model

Sample	Toluene			Acetone		
	q_e (mg/g _{ads})	k_2 (min ⁻¹)	R^2	q_e (mg/g _{ads})	k_2 (min ⁻¹)	R^2
NM-Si	269	3.00×10^{-5}	0.9953	347	1.47×10^{-5}	0.9966
NM-Ti-84	274	2.90×10^{-5}	0.9959	321	1.76×10^{-5}	0.9866
NM-Ti/Al	190	6.75×10^{-5}	0.9937	365	1.33×10^{-5}	0.9879
NM-Al-87	166	9.54×10^{-5}	0.9925	401	1.09×10^{-5}	0.9966
NM-Al-41	162	9.47×10^{-5}	0.9944	250	2.99×10^{-5}	0.9972
CM-Al-23	124	1.62×10^{-4}	0.9928	202	4.70×10^{-5}	0.9966

Table S8. Kinetic data and correlation coefficient R^2 obtained from Elovich model

Sample	Toluene			Acetone		
	a	b	R^2	a	b	R^2
	($\text{mg}/\text{g}_{\text{ads}} \cdot \text{min}^{-1}$)	($\text{g}_{\text{ads}}/\text{mg}$)		($\text{mg}/\text{g}_{\text{ads}} \cdot \text{min}^{-1}$)	($\text{g}_{\text{ads}}/\text{mg}$)	
NM-Si	5.08	0.021	0.9951	5.85	0.029	0.8923
NM-Ti-84	5.08	0.021	0.9957	5.86	0.028	0.8969
NM-Ti/Al	5.16	0.024	0.9946	5.88	0.028	0.8912
NM-Al-87	5.21	0.025	0.9942	4.49	0.018	0.9939
NM-Al-41	5.08	0.028	0.9959	4.44	0.023	0.9960
CM-Al-23	5.04	0.035	0.9947	5.63	0.036	0.9174

References

- [1] L. Cáceres, M. Escudey, E. Fuentes, M.E. Báez, *Journal of Hazardous Materials*, 2010, 179, 795-803.
- [2] A.K. Nayak, A. Pal, *Journal of Molecular Liquids*, 2019, 276, 67-77.
- [3] Y.S. Ho, G. McKay, *Process Biochemistry*, 1999, 34, 451-465.
- [4] G. Skodras, I. Diamantopoulou, G. Pantoleontos, G.P. Sakellariopoulos, *Journal of Hazardous Materials*, 2008, 158, 1-13.